Anatomical distribution of lipids in human brain cortex by imaging mass spectrometry

Antonio Veloso,[1] Egoitz Astigarraga,[1] Gabriel Barreda-Gómez,[2] Iván Manuel,[2] Isidro Ferrer,[4] María Teresa Giralt,[2] Begoña Ochoa,[3] Olatz Fresnedo,[3] Rafael Rodríguez-Puertas,[2] José A. Fernández.[1]

[1]Department of Chemical Physics, Faculty of Science and Technology.

[2]Department of Pharmacology; [3]Department of Physiology; Faculty of Medicine and Dentistry.

University of the Basque Country, Sarriena s/n, 48940 Leioa, Spain

[4]Institute of Neuropathology, IDIBELL-University Hospital Bellvitge, Hospitalet de Llobregat; Centro de Investigación Biomédica en Red de Enfermedades Neurodegenerativas CIBERNED; Spain.

TITLE RUNNING HEAD: lipids in human brain

Address reprint requests to Dr. José A. Fernández, Dpto. Química Física, Fac. Ciencia y Tecnología, Universidad del País Vasco, bº Sarriena, s/n, 48940 Leioa, Spain. E-mail: josea.fernandez@ehu.es, Tel: +3494 601 5387; Fax: +3494 601 3500

Abbreviations

DAG, diacylglycerols; GPCho, glycerophosphocholines; GPEtn, glycerophosphoethanolamines; GPG, glycerophosphoglycerols; GPIns, glycerophosphoinositols; GPSer, glycerophosphoserines; IMS, imaging mass spectrometry; MALDI, matrix-assisted laser desorption/ionization; TLC: thin layer chromatography; TOF, time of flight; MBT, 2-mercaptobenzothiazole; SPM, sphingomyelins; ST, sulfatides; TAG, triacylglycerols; MS, mass spectrometry; PLSA: probabilistic latent semantic analysis; EDA: exploratory data analysis; PCA: principal component analysis; ICA: independent component analysis; LSA: latent semantic analysis; SVD: singular value decomposition; CLP: cardiolipin; CE, cholesteryl ester; Cer, ceramide; CNS, central nervous system.

ABSTRACT

Molecular mass images of tissues will be biased if differences in the physicochemical properties of the microenvironment affect the intensity of the spectra. To solve this issue we have performed, by means of MALDI-TOF mass spectrometry, imaging on slices and lipidomic analysis in extracts of frontal cortex, both from the same postmortem tissue samples of human brain. An external calibration was used to achieve a mass accuracy of ~10 ppm in the spectra of the extracts, allowing us to propose identification for ~150 different lipid species (m/z from 400 to 1600), thereby increasing considerably the knowledge of the lipid composition of human brain. The spectra recorded directly from tissue slices (imaging) show an excellent s/n ratio, almost comparable to ratios obtained from the extracts. In addition, they retain the information about the anatomical distribution of the molecular species present in autopsied frozen tissue. The comparison between the spectra from lipid extracts devoid of proteins and those recorded directly from the tissue, show unambiguously that the differences in lipid composition between gray and white matter observed in the mass images are not an artifact due to microenvironmental influences of each anatomical area in the signal intensity, but of a real variation in the lipid composition.

KEYWORDS: Imaging mass spectrometry, lipid profiling, *in situ* analysis, MALDI-TOF, human postmortem brain, thin layer chromatography.

I. Introduction

Mass spectrometry (MS) is an excellent tool for the analysis of the lipidome, due to its intrinsic characteristics:[1;2] fast acquisition times, robustness, high tolerance to impurities, and high dynamic range (from pmol/μl to mmol/μl). Therefore, an increasing number of studies have been published over the last few years, aiming at the identification of lipids in biological samples, using different mass spectrometry techniques.[3-6] The MALDI imaging mass spectrometry (IMS) technique, introduced by Caprioli et al.,[7;8] permits the scanning of tissue slices directly in the mass spectrometer, and therefore, takes the precise anatomical localization of different types of lipids a step further. Such information, which is lost in the extracts, is of singular importance to understand the physiopathology of the different lipid species, and more significant in the case of the central nervous system (CNS), which is composed of a network of very specialized groups of cells and signaling pathways distributed in discrete areas or nuclei of the brain.

Despite the potential applicability of this method and the growing number of papers published recently in the field of lipid IMS,[9-11] some questions remain unanswered and numerous concerns have been raised . Most importantly, it is not clear whether the difference in the intensity of lipid signals in different tissues or areas of a tissue is actually due to real differences in lipid concentrations or rather to changes in the environment from which the lipids are extracted during the desorption process.[12;13] Because of the nature of biological tissues, lipid signals might be affected by the presence of and/or the interaction with other lipids, proteins, salts and many other complex biological materials, such as nucleic acids or porphyrins. Given the tissue specificity of both composition and regional and subcellular organization of biomolecules, ionization efficiency is likely to be tissue-specific.

The improvement in sample preparation protocols for IMS[14] and the employment of new matrices[6] have made it possible to obtain spectra directly from tissues, with a s/n ratio and a resolution almost comparable to those obtained from lipid extracts.[10] Such improvements

allow us to determine if lipid extraction procedures preserve lipid concentration in the tissues, or if this is modified by differences in the lipids' physical-chemical properties, which result in different extraction ratios.

The present study also involves a proposal for the identification of a high number of lipid molecular species in frontal cortex samples of the human brain from *postmortem* tissue obtained from autopsies, and to provide information on the relative abundance and distribution of the identified species. To carry out a study of this nature, it is necessary to ensure that the original lipid composition is preserved during the extraction protocol and that mass distribution images reflect a real distribution of the different lipid species on the tissue. In addition, it is necessary to implement a protocol that allows one to obtain a clear correlation between signal distribution and density distribution in IMS experiments. The employment of this technique will be of enormous value in clarifying the physiological role of lipids, not only in the CNS, but also in pathological conditions, including devastating neurodegenerative diseases that affect an increasing number of patients worldwide.

The availability of data from both extracts and IMS of human brain postmortem tissue helped us to address some of the questions raised above. We prepared separate lipid extracts from gray and white matter of human frontal cortex that were compared with consecutive slices from the same samples. The anatomical distribution was analyzed with counter-stained slices and MALDI-IMS maps of molecular densities at different resolutions, obtaining over a hundred molecular lipid species. Moreover, we assigned over 150 lipid species on the mass spectra from the extracts, which were confirmed by analysis of separated classes. Additionally, we performed a lipid separation using thin layer chromatography TLC, in order to eliminate the signal interference between lipids in the mass spectra. The present work offers new and important information on the lipidome of human brain, which contributes to increase the knowledge of this subject.[6;15-20] In addition, the procedure used, comparing results from extracts of all lipid classes (lipid extracts), individual lipid classes (TLC) and

tissue slices from human brain cortex, provides an excellent approach with which to check for the ability of IMS to determine the anatomical distribution of lipid species in tissues at a few μm resolution, a necessary step prior to elucidating their physiological role.

II Experimental Procedures

Brain sectioning and lipid extraction

Samples were obtained from the Brain Bank of the Institute of Neuropathology (University Hospital Bellvitge, Barcelona). Human brains were obtained by autopsy after prior informed consent of the patients or their relatives and with the institutional approval of the ethics committees of the University Hospital Bellvitge and the University of the Basque Country. The samples were obtained from two male subjects (54 and 64 years old) who died suddenly after cardiac infarction and who had shown no evidence of neurological or metabolic disease. The neuropathological study disclosed no abnormalities in the brain. The interval between death and autopsy was 3 and 11 hours respectively. Following autopsy, the brain samples were immediately frozen at –80 ºC. The frozen tissue was brought to -25 ºC and 20 μm thick slices were obtained in a cryostat (Microm, HM550). Two consecutive sections were mounted on conducting slides (standard size slides for microscope, Bruker Daltonics) and kept at -25 ºC until they were introduced into a MALDI metal holder (Bruker Daltonics). A section consecutive to those on the slides was counter-stained with tionine, and a human brain atlas was used for the identification of the different cortical layers analyzed by MS. Around 100 mg of both gray and white matter samples from the same tissue sample were dissected and homogenized at 4 ºC in 5 vol. ice-cold phosphate buffer solution pH 7.4 using a Polytron (Kinematica) homogenizer. The protein content of the samples was comparable and was estimated in 5 mg protein/100 mg tissue using Pierce reagent.[21] Lipids were exhaustively extracted from homogenates by a modified Bligh and Dyer procedure described

earlier;[22] with an extraction efficiency of lipid classes of 95-99% according to radiometric analysis (data not shown). The solvent was removed in a Savant SpeedVac concentrator-evaporator, the lipids were dissolved in toluene, and the extracts were stored under N_2 atmosphere at -80 ºC until analyzed.

Thin Layer Chromatography

TLC of the lipid extracts from both gray and white matter was carried out on silica gel plates (aluminium sheets 5 x 7.5 mm Merk 60 RP-18 F254S) as described by Murata el at.[23] using the following mobile phases: chloroform/methanol/water (65:40:5, v/v/v), ethyl acetate/isopropanol/methanol/ethanol/chloroform/KCl 0.25% (35:5:15:20:22:9 v/v/v/v/v/v), n-heptane/diisopropyl ether/acetic acid (7:3:0.2 v/v/v) and n-heptane. The correct separation of the different classes of lipids was confirmed by the visualization with UV light (254 nm), using primuline. Two microliters of sample were used on each analysis (an overall lipid mass of about 20 μg). Separated spectra of the main lipid classes: GPCho, GPEtn and SPM were obtained using MBT as matrix, with the spectrometer working in reflectron mode. The laser energy was set at 70% in order to obtain an acceptable s/n ratio.

Sample preparation for MALDI-TOF and IMS

A saturated solution of MBT (Sigma-Aldrich, St. Louis, MO) in methanol was employed as matrix solution both for extracts and tissues as described previously.[9] Lipid extracts with a total lipid concentration of ~10 mg/ml were mixed with the matrix solution in a 1:10 (v/v) ratio in order to adjust total lipid concentration to ca. 1 mg/ml. One μl of the mixture was spotted in each well of the stainless steel target plate and co-crystallized by evaporation. To obtain the constants of the external calibration polynomial, 36 peaks of the polyethylene glycol-sodium adduct $[PEG\text{-}Na]^+$ spectrum in the range 400-2000 Da, obtained in various positions of the target plate surrounding the sample, were used and fitted to 15-25 degree

polynomials, with the 19-degree polynomial providing the best fit. In this way, an ~10 ppm accuracy in mass determination was achieved.[9]

Spectra were acquired in either positive or negative linear and reflectron modes with the aid of a Bruker (Bremen, Germany) Reflex IV time-of-flight mass spectrometer, employing different sets of voltages for the ion source in order to focus the adequate mass range. 900 shots were accumulated for each spectrum of extracts, and at least 10 replicates of each extract were analyzed to assess reproducibility of the spectra.

In the IMS experiments, a uniform coat of matrix was applied using a sprayer (DESAGA, model SG1B), loaded with an MBT/methanol saturated solution. The matrix was sprayed from a 50 cm distance, exposing the sample only when the sprayer was in stationary regimen. Up to 20 spraying/drying cycles were employed in order to obtain a uniform layer. With this technique it was demonstrated that resolutions of at least 50 μm can be achieved.[9]

The definition of the acquisition area was performed with the CreateTarget computer software,[24] generating files in a format compatible with the Bruker Reflex IV spectrometer. 30 shots on each single location were accumulated to construct each individual spectrum, with a total acquisition time of 2-9 hours, depending on the size of the scanned area. The spatial resolution of the mass images shown in the present study varies from 50 to 200 μm. As there is a shift in the masses across the tissue, acquired spectra were aligned maximizing correlation with the overall averaged spectrum, normalized by using the total ion current and exported to the computer program Histomass™ in a compatible format using a script written in Mathematica™ 6.0. The data analysis and visualization were carried out with Histomass™, a powerful computer program created specifically for the graphical evaluation of data from IMS experiments (http://www.noraybio.com/en/histomass.asp).

Probabilistic Latent Semantic Analysis (PLSA)

The data from the IMS experiments were analyzed using a modified version of the PLSA algorithm.[25] The PLSA is preferred over other commonly employed exploratory analysis techniques, like PCA (principal component analysis) or ICA (independent component analysis), because it does not yield negative values, which are difficult to interpret. However, the results from the PLSA depend on the number of iterations and on the initialization values. To circumvent such drawbacks, we employed an LSA (latent semantic analysis) algorithm to create a set of initial parameters, which were further refined using an expectation maximization algorithm. The LSA consists of decomposing the matrix formed by the mass channels on the spectra into singular values (SVD),[26;27] which can be defined as a probability model. The resulting matrices are a more robust set of initializing vectors for the PLSA model. In summary, the LSA-PLSA method provides a non-negative decomposition of the IMS data matrix, which is easy to interpret, of good quality and independent of the initial conditions. All the algorithms were implemented in Mathematica™ 6.0, using precompiled instructions in order to increase the speed of the probabilistic analysis procedure.

Peak assignment

The human brain samples analyzed in this paper are quite complex, containing a large number of lipids that share similar masses. Without using MS/MS it is not possible to discriminate among chemical variants of lipids with identical numbers of acylic carbons and double bonds; that is, with identical masses. Therefore, the identity of the alkyl chains and the position of their double bonds could not be specified in this study. The assignment of lipid species was facilitated by the use of a database, which we created based on the specific lipid composition of the tissues. The experimental values of the peaks' positions were compared with this database and with the data in Lipid MAPS (http://www.lipidmaps.org/)

and Madison Metabolomics Consortium (http:mmcd.nmrfam.wisc.edu/) databases, using mass-accuracy as the tolerance window. A single candidate for each peak in the spectrum was obtained in most cases. The glycerolipid species numbers (x:y) denote the total length and number of double bonds of acyl chains, while the sphingolipid and sulfatide species numbers correspond to the length and number of double bonds of the acyl chain added to those of the attached sphing-4-enine (d18:1) or sphinganine (d18:0) base.

III. Results and Discussion

Serial sections from human brain samples of the frontal cortex (area 8) were obtained, and two of the sections were covered with MBT, following the procedure described above. A third section was stained to distinguish the different layers of the frontal cortex and the white matter. Simultaneously, two different portions (~5 mg protein/100 mg tissue) of the sample were processed following the methodology described to extract the lipids from gray and white matter separately.

Figure 1 shows a comparison between the stained section and the images obtained by using the IMS method representing single mass channels in individual images. In this figure, some representative lipid specie, together with the proposed assignment, are shown. The signal intensity is represented by the black-green-yellow color contrast of some mass channels against the spatial coordinates at which the spectra were acquired. Another additional image represents the three main components obtained from the LSA-PLSA analysis and this is shown in three different colors. The algorithm clearly groups the spectra in three differentiated regions: one corresponding to the areas where there is only matrix (in white), another area corresponding to the gray matter (in blue) and a third region corresponding to the white matter (in red). Accordingly, the IMS images, in black-green-yellow scale, show that the diverse lipid molecular species found in human brain cortex exhibit a different and

specific distribution; while some lipid species are evenly distributed along the whole section, like GPCho 34:1, SPM 36:1, or GPEt 38:1; others show a strong propensity to appear either in white matter (like GPCho 36:2 and GPEt 36:1) or in gray matter (like GPCho 32:0 and GPCho 38:6). Two different areas of the section in Figure 1 were scanned at a 50 μm resolution, that should be enough to distinguish between the six different layers of the cortex (see Figure S1, in the SI), finding slight differences in lipid density along the cortex. The cortical layers differ, mainly, in the type of neurons and fiber projections (dendrites and axons). The differences in lipid compossition between these layers (I-VI) are not as clear as they are for white and gray matter. However, it is also very probable that the 50 μm resolution is close to our experimental resolution limit.

The same section was employed to record averaged spectra over white and gray matter separately (900 shots per spectrum, Figure 2), prior to recording the results that are shown in Figure 1. This means that during the ca. 48 hours that the section was inside the spectrometer, which was the time taken to record the three scans and the averaged spectra, there was no degradation of the lipids or variation of the signal intensity due to matrix sublimation. This result is demonstrated by the comparison of the IMS images in Figures 1 and S1 with those in Figure S2, obtained from the sequential section, scanned at 100 μm resolution, and by comparing the spectra obtained from the tissue in each IMS experiment that were almost identical (data not shown).

The assignment of the mass channels represented in Figure 1 was performed by comparing the spectra recorded from the tissue with the assigned spectra of the extract, which were recalibrated with a polymer following the external calibration protocol described in Section II. Figure S3 (Supporting information) offers a detailed comparison between the spectra of one of the samples and that obtained from the extracts, together with two spectra that correspond to single locations (x:y coordinates) on the tissue section that are from white and gray matter respectively. The spectra resulting from gray matter are very similar in terms of

the relative abundance of the different lipid species, and this was also the case for the white matter. The intensity was higher in the extracts, but they correspond to the accumulation of 900 shots instead of the 30 used in each slice coordinate. Nevertheless, 30 shots were enough to get a good s/n ratio (see Figure S3), not very different from that on the extracts.

Table S1 (supporting information) lists the lipid species identified in the extracts. We propose an assignment for over 150 lipid species, although for some of them it was not possible to discriminate between several molecule candidates due to the similarity of their masses. Such an analytical refinement to assign the m/z values to a specific molecule (e.g. determine the fatty acid composition for glycerophospholipid species) with certainty, could be reached using an additional technique, such as MS/MS TOF, but this was out of the scope of the present study.

Figure 2 shows a comparison between the 710-840 Da region of the spectra, where the strongest signals appear, obtained from both the extracts of gray and white matter (upper traces) and the averaged spectra of 900 shots (in groups of 30 shots per location), recorded directly from gray and white matter from tissue slices (lower traces). The s/n ratio of the spectra recorded directly from the tissue is almost as good as that on the spectra from the extract, although the signal intensity is approximately one order or magnitude lower: 6500 counts compared with over 40000 counts.

Additionally, the average of the spectra classified using the LSA-PLSA probabilistic analysis shows an improved s/n ratio, equivalent to that obtained from the extracts (Figure 3). The comparison between the gray and white matter spectra from extracts shows, for example, changes in the relative intensity of GPCho 32:0, GPCho 38:6, GPEt 38:6 and most of the identified CLP species (Figures S1-S3), which are more abundant in gray matter. Meanwhile, other species such as GPCho 36:2, GPG 40:4 and TAG 52:6 are found predominantly in white matter. Nevertheless, we did not find that any of the identified species were exclusively

located in one of these main regions or matter of the sections. The differences correlate with different density distributions along the tissue. For example, the peak at 734.560 Da corresponding to GPCho 32:0+H^+ is more intense in the spectrum from the gray matter extract than in the white matter extract, in close agreement with the IMS presented in Figure 1, and with the differences observed between the averaged spectra recorded directly from the tissue. Also, the peak at 774.579 Da assigned as GPEtn 38:1+H^+ is more intense in the white matter spectra (both in extracts and tissue) than in the corresponding gray matter spectrum. A detailed view of that region of the mass spectrum is offered in Figure S3. From the above, one can conclude that the distribution maps obtained using IMS correspond to real variations in the lipid concentrations and that they are not due to changes in the environmental features of the anatomical areas that are analyzed.

The IMS experiments carried out directly in the tissue slices offer a second advantage: the absence of “hot spots” that can influence the relative intensity of the peaks. Furthermore, if an algorithm like the LSA-PLSA used here is employed, it is possible to identify not only the spectra of each region and to average them, but also to identify different regions, attending to the most common molecules that are present. The results are spectra representative of the relative concentrations of the molecules in the tissue and a greatly improved s/n ratio. Thus, the average spectra in Figure 3 show an excellent s/n ratio, comparable to, or even better than, those obtained from extracts (Figure 2). The insert in Figure 3 shows a detailed view of the 803-840 Da region of the average spectrum over the white matter to emphasize this point. The comparison between the spectra in Figures 2 and 3 makes it clear that the differences in distribution of the different lipid species found in the IMS experiments are not due to artifacts inherent to the technique. For example, the peaks in the region around 830 Da on the average spectrum of the gray matter in Figure 3 are weaker than in white matter. The predominant peak in that region is at 826.565 Da. and is assigned as GPCho 36:1+K^+ (see Figure S3), and is accompanied in the spectra from the tissue presented in Figure 2 by some

other peaks for which no satisfactory assignment was found. In summary, most of the differences between the spectra from extracts and from the LSA-PLSA average are due to differences in the abundance of adducts and to the existence of non-lipid species in the tissue slices. Consequently, a representative spectrum of each region of the tissue is obtained by applying a mathematical procedure to get the averaged spectrum.

An additional experiment was carried out to test the existence of ion suppression between lipids. It is well known, that the classes with quaternary amines (for example GPCho) yield a stronger signal, even at lower concentrations than other lipid species. The different abundance of such charged species in the two types of tissues (white or gray matter) in our samples could lead to a different detection of the rest of the lipids, even if they are in similar abundance. Thus, we applied the TLC separation protocol to samples of lipid extracts from white and gray matter and then recorded the MALDI spectra of three main classes of lipids on the sample: GPCho, GPEtn and SPM. The resulting spectra (Figs. S4-S6, supporting information) show an excellent agreement with the IMS results. For example, a clear increase in the intensity of the GPCho 32:0 is observed from white to gray matter, while the GPCho 36:1 exhibits the opposite trend. Also, it is clear from Fig. S5 that the overall amount of GPEtn is considerably larger in white matter than in gray matter. Finally, while SPM 36:1 concentration does not vary greatly from white to gray matter, there is a subtle decrease in SPM 34:1, in agreement with that observed in the IMS experiments.

In a recent paper, Goto-Inoue et al.[28] applied a TLC-Blot-MALDI-IMS procedure to lipid extracts from human frontal gyrus white and gray matter and hippocampus white and gray matter, and analyzed the differences in lipid composition for GPCho and SPM species. They found that the main GPCho peak corresponds to the 34:1 species, and also identified 32:0 and 36:1 in the mixture. They also report the identification of SPM 34:1, 36:1 38:1 and 42:2 species in the extracts. The analysis of the relative concentration of SPM in white and gray matter lead them to conclude that SPM 36:1 is in similar abundance in both types of matter,

while SPM 38:1 is more abundant in gray matter and SPM 42:2 is more abundant in white matter. If we compare the results from Goto-Inoue et al with those reported in this paper (Figs. S4-S6), they are similar except for the SPM 38:1 white/gray relative abundance. In our samples, we find the opposite trend to what is reported by Goto-Inoue. A possible reason for this difference may be that while they study the hippocampus, our samples are from the frontal cortex.

Despite the fact that little is known about human lipid species distribution and composition, our results are in accordance with others previously reported. In this context, it has been demonstrated [19;29;30] that human brain is mainly composed by cholesterol and phospholipids. Among the latter, the most abundant classes are GPCho, GPEtn and SPM, which are precisely the most detected species in the present work. Using LC/ESI, Isaac et al. determined the presence of GPCho 38:6, 36:4, 34:1 and 36:1, and SM 34:1, 36:1 and 42:2 species in human mesencephalon.[30] All of them were detected in the present study, and the GPCho species exhibit a strong signal. Moreover, O'Brien et al. determined the relative abundance of some phospholipid species between gray and white matter in human brain,[19] concluding that the SPM species are more abundant in white matter. We also observe a tendency of some of the SM species to be located in white matter (Figs. 1, S1 and S2). Söderberg et al. reached the same conclusion, but in addition, they estimated a phosphatidylethanolamine/ phosphatidilcholine (GPEtn/GPCho) ratio of ~ 1.7 for white matter and of 0.8 for gray matter,[31] in agreement with the present work, in which GPEtn is more abundant in white matter.

Some recent studies using MALDI-MS and MALDI-IMS have determined the distribution of several lipid species in rat brain.[9;32-35] In all these studies, a difference in lipid abundance between white and gray matter has been observed. For example, Woods et al., using DHA matrix obtained spectra from cerebellar cortex and peduncule (i.e., gray and white matter) of rats, and, among the species identified, those yielding the strongest signal were GPCho 30:0,

34:1 and 36:1 and SPM 36:1, which are also the species that give the strongest signal in the spectra shown in the present study. Furthermore, their study points to a higher abundance of GPCho 32:0 in gray matter, while GPCho 36:1 is more abundant in white matter. We observed the same relative abundance in the human samples, as depicted in Figs. 1, S1 and S2. Woods et al. also used the ion mobility method to study some additional cerebral areas,[36;34] observing a different distribution of diverse phospholipid species. For example, while GPCho 34:1 is distributed uniformly along the tissue, GPCho 32:0 is more abundant in white matter and GPCho 38:6 is more abundant in gray matter, as has also been observed in the present work. The same tendency was observed by Jackson et al. using colloidal graphite as matrix.[35]

In summary, all of the above cited studies report that while some lipid species are evenly distributed, others are more abundant in one type of matter and although different techniques and matrices were used, their results are in agreement with the results we have obtained.

The present study describes a precise distribution of the different lipid species within white and/or gray matter of the human frontal cortex, area 8. The differences in the relative abundance of each specific lipid molecule must be related to different physiological roles. In this sense, there are virtually no neurons in white matter, which is mainly formed by glial cells and the “wiring” of the brain, the axons, that are isolated by the myelin envelopment enriched in saturated fatty acids. Moreover, it is known that the lipid/protein ratio is higher for the white matter, and that GPIns or GPCho are not only essential for the integrity of the membranes, but also for intracellular signaling processes.[37] However, the anatomical localization of precise molecules by IMS in the brain is already generating new questions related to what this specific localization means in relation to the functions of specific lipids in the brain and in different diseases affecting the CNS.

Conclusions

In this study we analyzed the lipid composition of the frontal cortex (area 8) from human brain postmortem samples, using both lipid extracts and IMS on frozen sections. The comparison between spectra from extracts and tissue slices points to a very efficient extraction protocol, which does not modify the original lipid composition. There is a clear difference in lipid composition between gray and white matter, both in extracts and in the tissue, demonstrating that the density maps represented in IMS experiments and obtained by probabilistic analysis correspond to real differences in the lipid composition of the different areas of the tissue. This is further confirmed by the spectra obtained from the different lipid classes separated using TLC. Such a conclusion opens the field to applying this IMS approach in the study of lipid distribution in different kinds of tissue samples, including frozen samples from human autopsies.

Acknowledgments

This study was supported by the Spanish Ministry of Education and Science (SAF2007-60211) and the Basque Government (PE06UN24 and IT-325-07), with grants to BO and OF, SAIOTEK SAI07/46, Biscay County Council (DIPE07/05), Carlos III Health Institute (FIS PI070628) and UPV/EHU GIU07/50. IM and AV are recipients of UPV/EHU graduate fellowships. GB is supported by a grant of the UPV/EHU Researchers Specialization Program.

Supporting Information

Additional information as noted in text. This material may be found in the online version at …

Reference List

1. Schiller, J.; Suss, R.; Fuchs, B.; Muller, M.; Zschornig, O.; Arnold, K. *Frontiers in Bioscience* **2007,** *12*, 2568-79.

2. Carrasco-Pancorbo, A.; Navas-Iglesias, N.; Cuadros-Rodriguez, L. *Trac-Trends in Analytical Chemistry* **2009,** *28*, 263-78.

3. Dennis, E. A. *Proceedings of the National Academy of Sciences of the United States of America* **2009,** *106*, 2089-90.

4. Bisogno, T.; Piscitelli, F.; Di Marzo, V. *European Journal of Lipid Science and Technology* **2009,** *111*, 53-63.

5. Han, X. L.; Jiang, X. T. *European Journal of Lipid Science and Technology* **2009,** *111*, 39-52.

6. Fuchs, B.; Schiller, J. *European Journal of Lipid Science and Technology* **2009,** *111*, 83-98.

7. Caprioli, R. M.; Farmer, T. B.; Gile, J. *Analytical Chemistry* **1997,** *69*, 4751-60.

8. Caprioli, R. M.; Farmer, T. B.; Zhang, H. Y.; Stoeckli, M. *Abstracts of Papers of the American Chemical Society* **1997,** *214*, 113-ANYL.

9. Astigarraga, E.; Barreda-Gomez, G.; Lombardero, L.; Fresnedo, O.; Castano, F.; Giralt, M. T.; Ochoa, B.; Rodriguez-Puertas, R.; Fernandez, J. A. *Analytical Chemistry* **2008,** *80*, 9105-14.

10. Chen, R. B.; Hui, L. M.; Sturm, R. M.; Li, L. J. *Journal of the American Society for Mass Spectrometry* **2009,** *20*, 1068-77.

11. Trim, P. J.; Atkinson, S. J.; Princivalle, A. P.; Marshall, P. S.; West, A.; Clench, M. R. *Rapid Communications in Mass Spectrometry* **2008,** *22*, 1503-09.

12. Murphy, R. C.; Hankin, J. A.; Barkley, R. M. *Journal of Lipid Research* **2009,** *50*, S317-S322.

13. Heeren, R. M. A.; Smith, D. F.; Stauber, J.; Kukrer-Kaletas, B.; MacAleese, L. *Journal of the American Society for Mass Spectrometry* **2009,** *20*, 1006-14.

14. Hankin, J. A.; Barkley, R. M.; Murphy, R. C. *Journal of the American Society for Mass Spectrometry* **2007,** *18*, 1646-52.

15. Kohler, M.; Machill, S.; Salzer, R.; Krafft, C. *Analytical and Bioanalytical Chemistry* **2009,** *393*, 1513-20.

16. Baek, R. C.; Martin, D. R.; Cox, N. R.; Seyfried, T. N. *Lipids* **2009,** *44*, 197-205.

17. Martinez, M.; Mougan, I. *Journal of Neurochemistry* **1998,** *71*, 2528-33.

18. Rouser, G.; Galli, G.; KRITCHEV.G *Pathologie Biologie* **1967,** *15*, 195.

19. Obrien, J. S.; Sampson, E. L. *Journal of Lipid Research* **1965,** *6*, 537.

20. Rouser, G.; Lieber, E.; Galli, C.; Kritchevsky, G.; Heller, D. *Federation Proceedings* **1964,** *23*, 228.

21. Pierce, J.; Suelter C. H. . *Anal. Biochem.*. **1977,** *81*, 478-80.

22. Ruiz, J. I.; Ochoa, B. *J Lipid Res* **1997,** *38*, 1482-89.

23. Murata, N.; Sato, N.; Omata, T.; Kuwabara, T. *Plant and Cell Physiology* **1981,** *22*, 855-66.

24. Clerens, S.; Ceuppens, R.; Arckens, L. *Rapid Communications in Mass Spectrometry* **2006,** *20*, 3061-66.

25. Hanselmann, M.; Kirchner, M.; Renard, B. Y.; Amstalden, E. R.; Glunde, K.; Heeren, R. M. A.; Hamprecht, F. A. *Analytical Chemistry* **2008,** *80*, 9649-58.

26. Ding, C. *Journal of the American Society for Information Science and Technology* **2005,** *56*, 597-608.

27. Ding, C. *Sigir'99: Proceedings of 22Nd International Conference on Research and Development in Information Retrieval* **1999,** 58-65.

28. Goto-Inoue, N.; Hayasaka, T.; Taki, T.; Gonzalez, T. V.; Setou, M. *Journal of Chromatography A* **2009,** *1216*, 7096-101.

29. Rouser, G.; Fleischer, S.; Yamamoto, A. *Lipids* **1970,** *5*, 494-96.

30. Isaac, G.; Bylund, D.; Mansson, J. E.; Markides, K. E.; Bergquist, J. *Journal of Neuroscience Methods* **2003,** *128*, 111-19.

31. Soderberg, M.; Edlund, C.; Kristensson, K.; Dallner, G. *Journal of Neurochemistry* **1990,** *54*, 415-23.

32. Woods, A. S.; Jackson, S. N. *Aaps Journal* **2006,** *8*, E391-E395.

33. Jackson, S. N.; Wang, H. Y. J.; Woods, A. S. *Journal of the American Society for Mass Spectrometry* **2005,** *16*, 2052-56.

34. Jackson, S. N.; Ugarov, M.; Egan, T.; Post, J. D.; Langlais, D.; Schultz, J. A.; Woods, A. S. *Journal of Mass Spectrometry* **2007,** *42*, 1093-98.

35. Cha, S. W.; Yeung, E. S. *Analytical Chemistry* **2007,** *79*, 2373-85.

36. Jackson, S. N.; Wang, H. Y. J.; Woods, A. S. *Journal of the American Society for Mass Spectrometry* **2007,** *18*, 17-26.

37. Farooqui, A. A.; Horrocks, L. A.; Farooqui, T. *Chemistry and Physics of Lipids* **2000,** *106*, 1-29.

Figure Captions

Figure 1. Distribution of some representative lipid species in a tissue section of frontal cortex from human brain, together with a consecutive stained section and the representation of the principal components identified by LSA-PLSA. The section was 20x15 mm and the spectra were recorded with 200 μm spacing, resulting in 7500 spectra. 30 shots were accumulated at each point with the spectrometer working in reflectron mode. Laser power was set at 55%. Tionine staining Bar dimensions 0.5 cm. The average spectra recorded by accumulating 900 shots along each type of matter are shown in Figure 2, while the average of each of the components is depicted in Figure 3. See Table 1 in supplementary material for the assignment of each m/z with a lipid molecule.

Figure 2. Comparison between mass spectra obtained from extract of lipids from human brain gray and white matter (upper traces), and the average spectra recorded directly from the tissue slice, selecting only either white or gray matter (lower traces). Each spectrum is the average of 900 shots along the tissue, with the laser power at 55% and using MBT matrix. Detection is performed in positive reflectron mode. Detailed views of the spectra with the assignment proposed can be found in Fig. S3 of the supporting information.

Figure 3. Comparison between the average of the 710-840 Da region of the spectra corresponding to the two components found in the LSA-PLSA analysis of the section in Figure 1. The insert shows a detail of the 803-840 Da region in which the excellent s/n ratio can be appreciated.

Figure 1

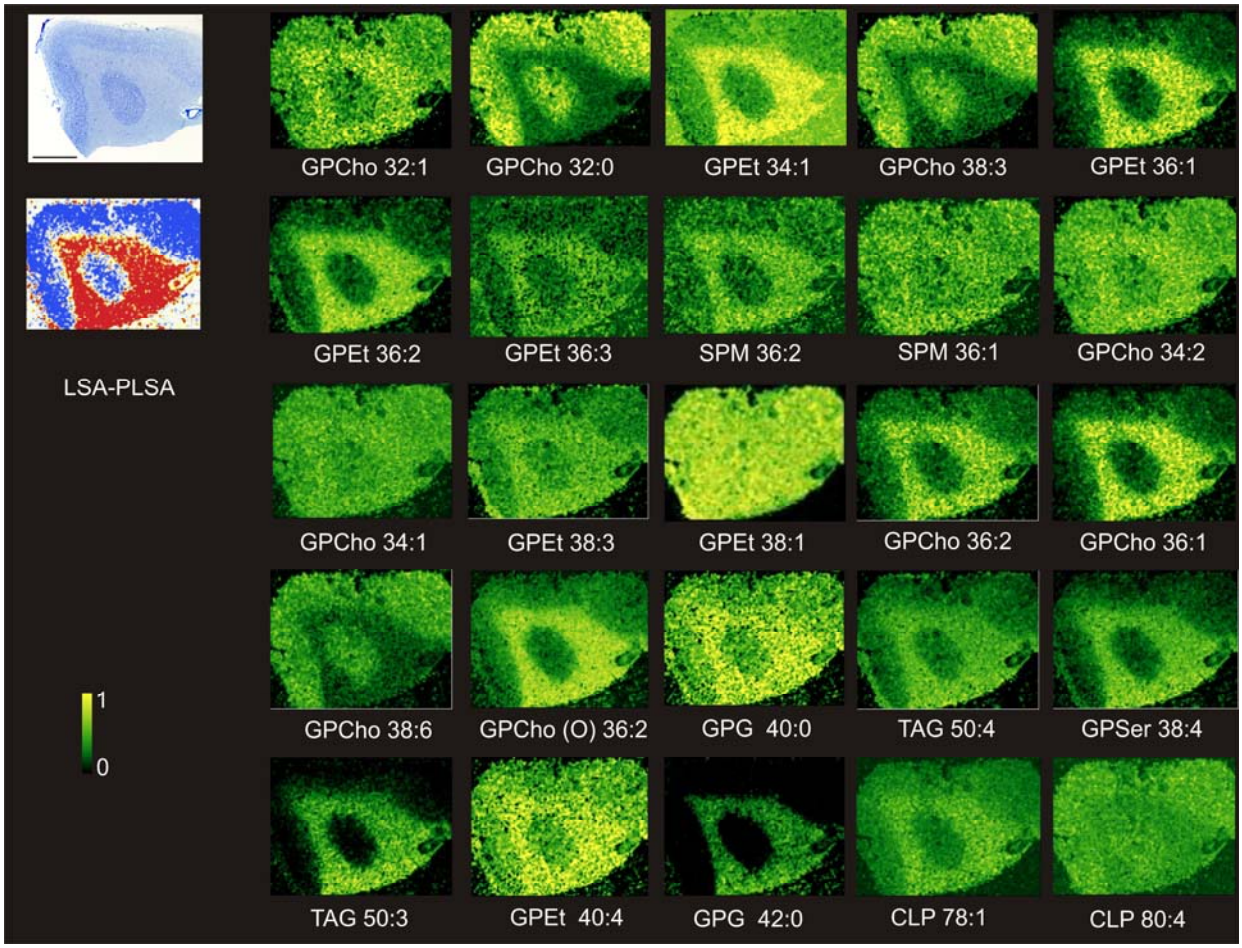
LSA-PLSA
1
0
GPCho 32:1
GPCho 32:0
GPEt 34:1
GPCho 38:3
GPEt 36:1
GPEt 36:2
GPEt 36:3
SPM 36:2
SPM 36:1
GPCho 34:2
GPCho 34:1
GPEt 38:3
GPEt 38:1
GPCho 36:2
GPCho 36:1
GPCho 38:6
GPCho (O) 36:2
GPG 40:0
TAG 50:4
GPSer 38:4
TAG 50:3
GPEt 40:4
GPG 42:0
CLP 78:1
CLP 80:4

Figure 2

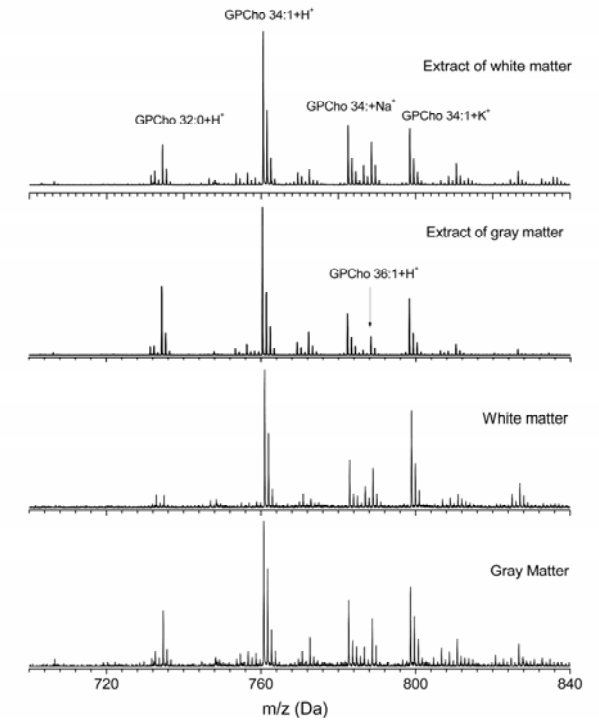
GPCho 34:1+H+
Extract of white matter
GPCho 32:0+H+
GPCho 34:+Na+
GPCho 34:1+K+
Extract of gray matter
GPCho 36:1+H+
White matter
Gray Matter
720
760
800
840
m/z (Da)

Figure 3

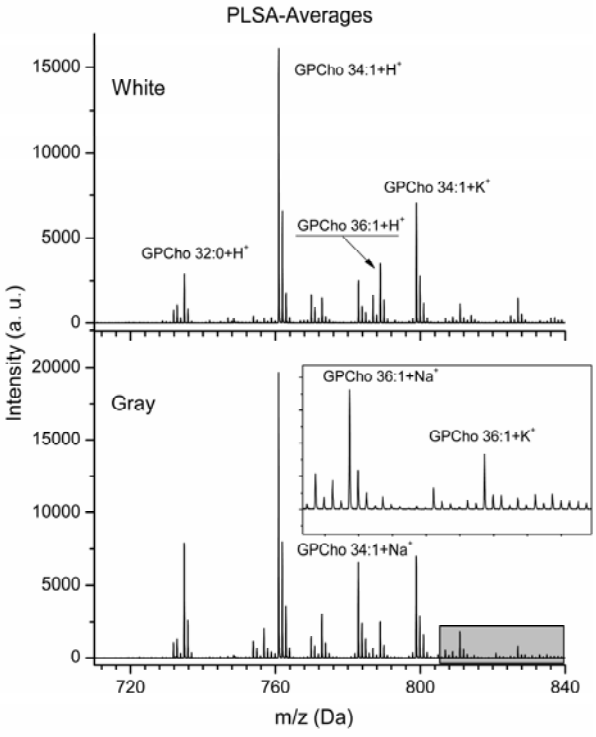
PLSA-Averages
White
GPCho 34:1+H+
GPCho 34:1+K+
GPCho 36:1+H+
GPCho 32:0+H+
Gray
GPCho 36:1+Na+
GPCho 36:1+K+
GPCho 34:1+Na+
Intensity (a. u.)
m/z (Da)
15000
10000
5000
0
20000
720
760
800
840

Figures

Click here to download high resolution image

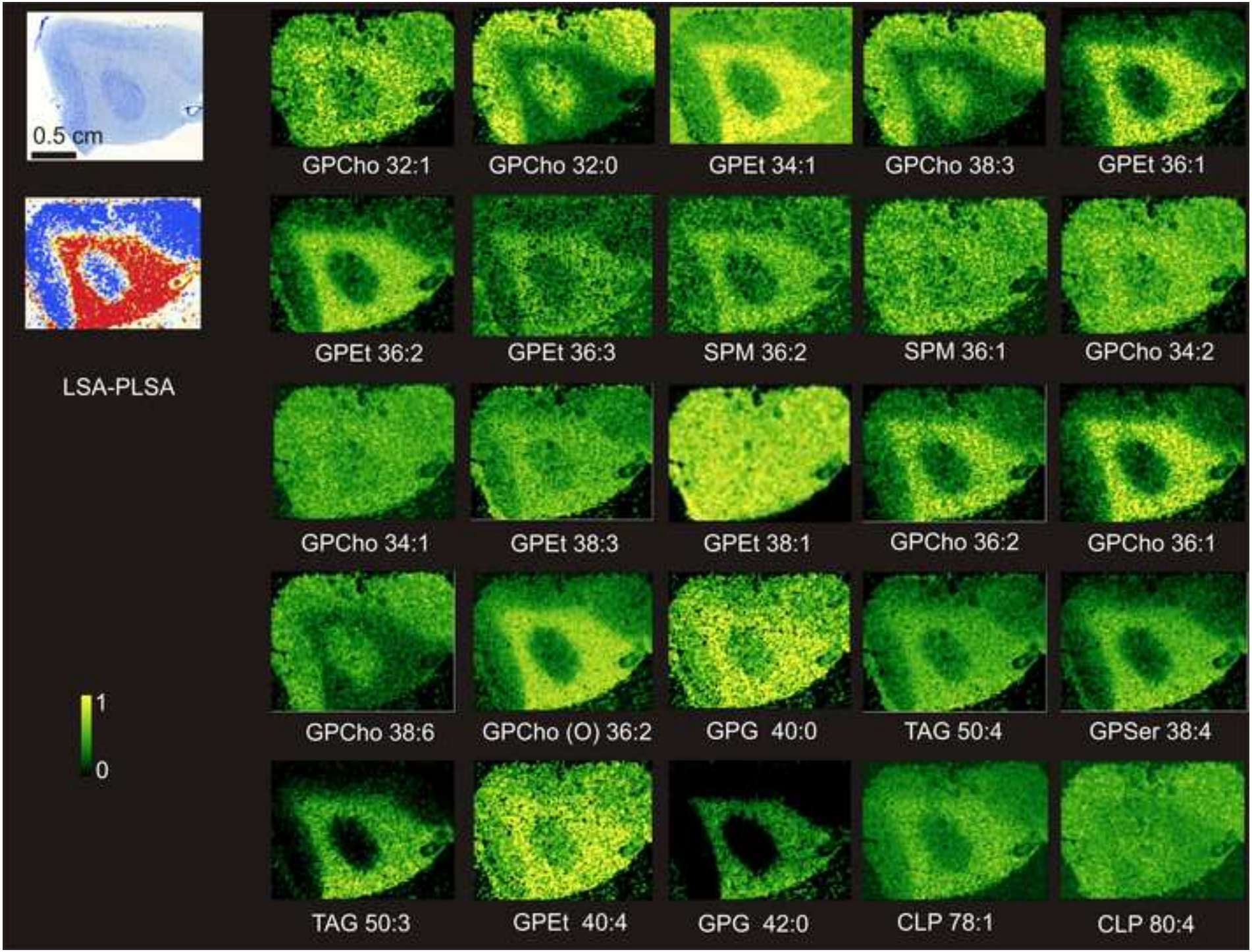

Figures

Click here to download high resolution image

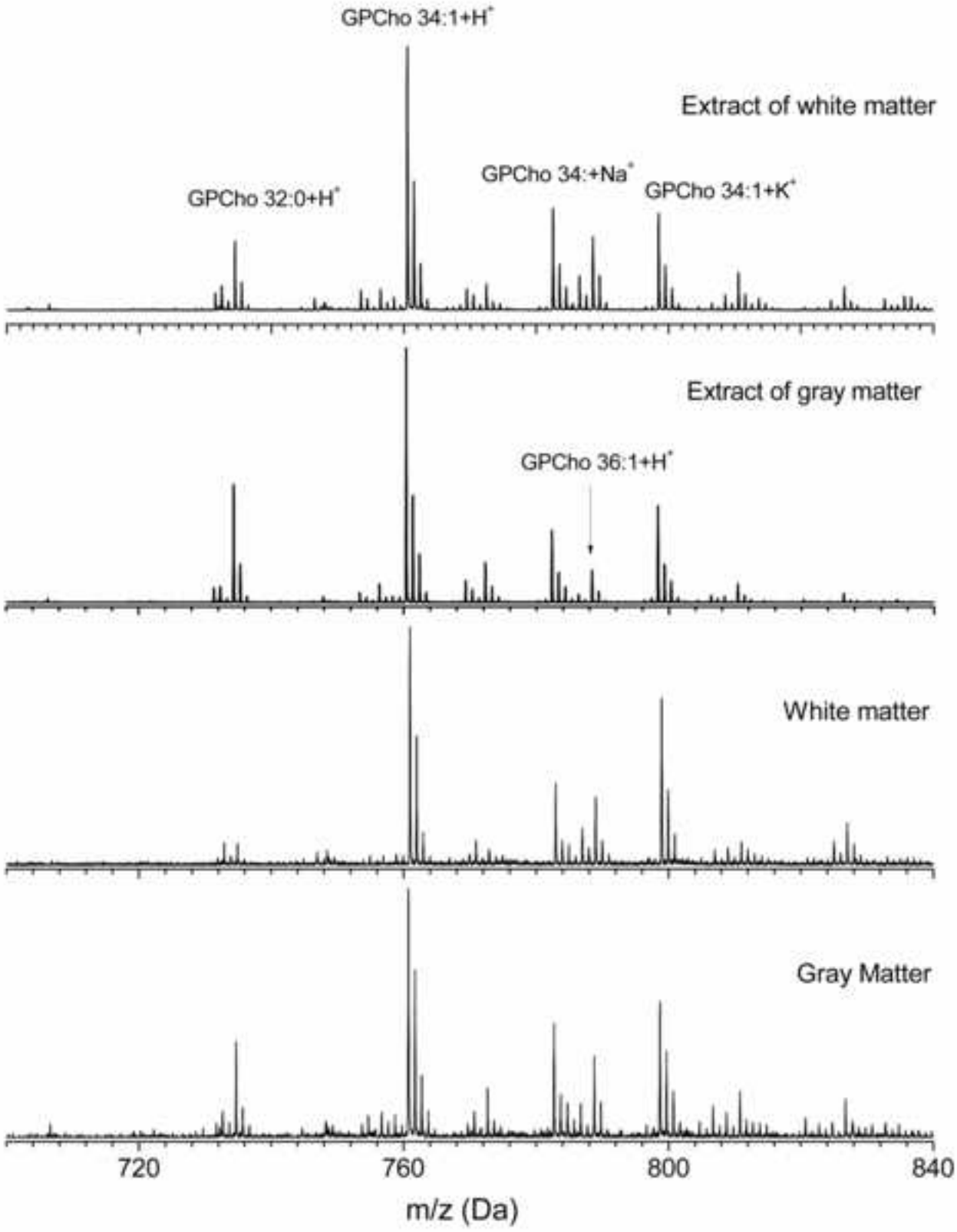

Figures

Click here to download high resolution image

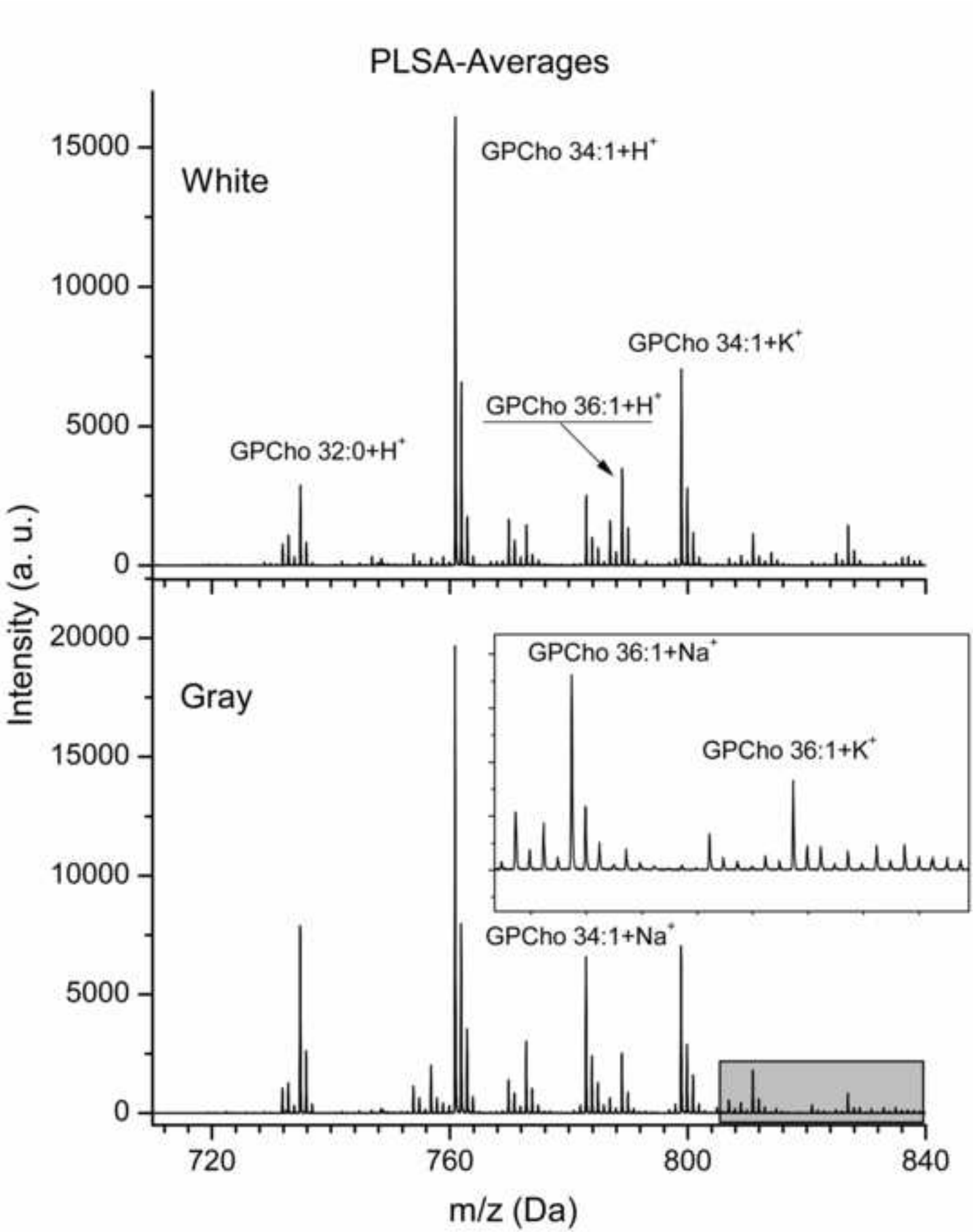

Supplemental Information

Click here to download Supplemental Information: LI03-Supporting Information-Lipids in human brain.doc